ORIGINAL ARTICLE

WILEY Cancer Science

DANCR-mediated microRNA-665 regulates proliferation and metastasis of cervical cancer through the ERK/SMAD pathway

Liyan Cao[1] | Haihong Jin[2] | Yue Zheng[3] | Yu Mao[1] | Zhanzhao Fu[1] |
Xin Li[1] | Lixin Dong[1] (iD)

[1]Department of Radiation Oncology, The First Hospital of Qinhuangdao, Qinhuangdao, China

[2]Department of Gynecology, The First Hospital of Qinhuangdao, Qinhuangdao, China

[3]Department of Gastroenterology, The First Hospital of Qinhuangdao, Qinhuangdao, China

Correspondence
Lixin Dong, Department of Radiation Oncology, The First Hospital of Qinhuangdao, Qinhuangdao, China.
Email: donglixin6447@sina.com

Funding information
Science and Technology Research and Development Plan of Hebei, Grant/Award Number: 162777146

Emerging evidence has indicated that microRNAs (miRNAs) play an important role in cervical cancer (CC). However, the role of miRNA (miR)-665 in cervical cancer remains unclear. The aim of the present study was to investigate the potential functions of miR-665 in CC and to identify the underlying mechanisms of action. Herein, we show that miR-665 was downregulated in CC tissues and cell lines, which is negatively correlated with tumor size, distant metastasis, advanced TNM stage and poor prognosis. Functionally, miR-665 inhibited cell proliferation, migration and invasion and resistance of cisplatin for CC cells, as well as tumor growth. We validated that transforming growth factor beta receptor 1 (TGFBR1) was a direct target of miR-665 and mediated the ERK/SMAD pathway. In addition, we identified miR-665 as the competing endogenous RNA for long noncoding (lnc)-DANCR. These observations suggested that lnc-DANCR-mediated miR-665 downregulation regulates the malignant phenotype of CC cells by targeting TGFBR1 through the ERK/SMAD pathway, which may present a pathway for novel therapeutic stratagems for CC therapy.

KEYWORDS
cervical cancer, DANCR, ERK/SMAD, miR-665, TGFBR1

1 | INTRODUCTION

Cervical cancer (CC) is the fourth leading cause of cancer death for women and the third most common malignancy in women worldwide, resulting in approximately 300 000 mortalities each year.[1-3] In 2015, according to Chinese cancer statistics, there were approximately 100 000 new cervical cancer cases and 30 000 mortalities as a result of cervical cancer.[4] In recent years, periodic cancer screening and prompt surgical treatment have increased; however, CC remains a public health concern worldwide because of the indistinct molecular mechanisms of its development and progression.

Long noncoding RNAs (lncRNAs) are nonprotein-coding RNA transcripts that exert a key role in many cellular processes and have potential toward addressing disease etiology.[5-7] Long noncoding RNA-DANCR is a valuable cancer-related lncRNA whose

dysregulated expression was found in a variety of malignancies, including bladder cancer, hepatocellular carcinoma, breast cancer, glioma, colorectal cancer, gastric cancer, osteosarcoma and lung cancer.[8] For example, DANCR played a critical regulatory role in bladder cancer cells and DANCR might serve as a potential diagnostic biomarker and therapeutic target of bladder cancer.[9] In addition, silencing DANCR was shown to efficiently impair colon tumor growth by promoting caspase 3 expression and tumor apoptosis.[10] Importantly, MYC-targeted DANCR promotes cancer, in part, by reducing p21 levels.[11]

MicroRNAs (miRNAs) are small noncoding RNAs of 18-22 nucleotides (nt) in length that are able to bind to the 3′-UTR of specific mRNA targets to regulate their translation at the post-transcriptional level.[12-14] Several previous studies have demonstrated that some miRNAs are dysregulated in many cancers, especially in CC.[15-17] For

example, miR-374b inhibited cell proliferation and induces apoptosis through the p38/ERK signaling pathway by binding to JAM-2 in cervical cancer.[18] In addition, miR-136 inhibited proliferation and promoted apoptosis and radiosensitivity of cervical carcinoma through the nuclear factor kappa B (NF-κB) pathway by targeting E2F1.[19] Furthermore, miR-346 functioned as a prosurvival factor under endoplasmic reticulum (ER) stress by activating mitophagy in CC cells.[20] However, the level and role of miR-665 in CC remains unclear.

In the present study, using deep-sequencing, The Cancer Genome Atlas (TCGA) and the OncomiR database, we found that miR-665 was downregulated in CC. The level of miR-665 was negatively correlated with tumor size, distant metastasis, advanced TNM stage and poor clinical prognosis. Function analysis showed that miR-665 overexpression inhibited cell proliferation in CC cells in vitro and tumor growth in vivo by directly targeting transforming growth factor beta receptor 1 (TGFBR1). Next, Transwell analysis showed that the inhibitive effect of miR-665 on cell migration and invasion occurred by blocking epithelial-mesenchymal transition (EMT) in CC cells by directly targeting TGFBR1. In addition, miR-665 overexpression also inhibited the cell cycle and drug resistance and promoted cell apoptosis by directly targeting TGFBR1. Furthermore, we found that miR-665 could inactivate the ERK/SMAD pathway by regulating TGFBR1. We then identified miR-665 as the competing endogenous RNA (ceRNA) for lnc-DANCR. Taken together, our results may provide a new insight into understanding the axis of DANCR-miR-665-ERK/SMAD in CC and this discovery could be a valuable target for developing therapies against CC.

2 | MATERIALS AND METHODS

2.1 | Human tissue sample collection

Thirty-three pairs (three random pairs for deep-sequencing; 30 pairs for RT-qPCR assay) of human cervical tissue, consisting of human CC and matched normal cervical tissue from the same patient, were used in this study. The samples were received from the Department of Gynecology, The First Hospital of Qinhuangdao from November 2017 to February 2018. The study was approved by the ethical review committees (Ethic Number: TFHQ2016213). Written informed consent was obtained from all enrolled patients, and all relevant investigations were carried out according to the principles of the Declaration of Helsinki.

2.2 | Deep sequencing

Total RNAs of three pairs of human CC and matched normal cervical tissue were isolated with TRIzol reagent (Sigma, St Louis, MO, USA) according to the manufacturer's instructions and were immediately frozen in liquid nitrogen and stored at −80°C. Deep-sequencing was carried out at Suzhou Basepair Biotechnology Corporation (Suzhou, China, http://www.basepair.cn/). Data analysis was done using Gene-Spring GX software 11.0 (Agilent Technologies, Santa Clara, CA, USA).

2.3 | Cell line culture and transfection

Endl/E6E7 and H8 were obtained from Shanghai Medical College, Fudan University, and cultured in KER-SFM medium supplemented with 10% calf serum (Gibco, Rockville, MD, USA) at 37°C with 5% CO_2. Other cervical cancer cells used in this study were obtained from ATCC (Manassas, VA, USA) and cultivated in RPMI 1640 or DMEM (Invitrogen, Carlsbad, CA, USA) supplemented with 10% FCS (Gibco), 100 U/mL penicillin and 100 µg/mL streptomycin (Solarbio, Beijing, China) at 37°C in a 5% CO_2 constant temperature incubator. Transfection assay was done using Lipofectamine 2000 reagent (Invitrogen) according to the protocol supplied by the manufacturer.

2.4 | RNA isolation and detection

Total RNAs of cells were extracted with TRIzol reagent (Sigma) according to the manufacturer's instructions. Quality and integrity of acquired RNA was evaluated by Nanodrop 2000c (Thermo Fisher Scientific, Carlsbad, CA, USA) and gel electrophoresis, respectively. For RT-qPCR, total RNAs were reversely transcribed with miScript II RT kit (Qiagen, Hilden, Germany). Real-time PCR was carried out using SYBR Premix Ex TaqTM II (Takara, Japan) on a Light Cycler (Roche Diagnostics, Roche, Minneapolis, MN, USA). Primers used were followed by: miR-665-RT, 5′GTCGTATCCAGTGCAGGGTCCGAGGTGCACTGGATACGACAG GGGC3′; miR-665-qPCR-Fwd, 5′TGCGGACCAGGAGGCTGAG3′; U6-RT, 5′GTCGTATCCAGTGCAGGGTCCGAGGTGCACTGGATACGACA AAATATGG3′; U6-qPCR-Fwd, 5′TGCGGGTGCTCGCTTCGGCAGC3′; miR-665-Rev, 5′CCAGTGCAGGGTCCGAGGT3′; OligodT, 5′TTTTTTT TTTTTTTTTTTT3′; TGFBR1-qPCR-Fwd, 5′AAAACATTATCGCAACTCA G3′; TGFBR1-qPCR-Rev, 5′CACAGAAAGGACCCACAT3′; β-actin-qPCR-Fwd, 5′CGTGACATTAAGGAGAAGCTG3′; β-actin-qPCR-Rev, 5′CTAGA AGCATTTGCGGTGGAC3′; DANCR-qPCR-Fwd, 5′GCGCCACTATGTA GCGGGTT3′; DANCR-qPCR-Rev, 5′TCAATGGCTTGTGCCTGTAGTT3′.

2.5 | MTT assay

HeLa and C33A cells were seeded into 96-well plates at 4500 cells per well 1 day prior to transfection as indicated. Cell viability at 48 and 72 hours post-transfection was determined by MTT assay (Dojindo Molecular Technologies, Inc., Kumamoto, Japan). Absorbance values at 570 nm were measured using the Quant Microplate Spectrophotometer (BioTek, Winooski, VT, USA).

2.6 | Colony formation assay

For the colony formation ability assay, HeLa and C33A cells were counted at 24 hours post-transfection and seeded into 24-well plates at 300 cells/well. Culture medium was replaced every 3 days. After ~2 weeks, cells were washed with PBS. Subsequently, colonies were fixed with 4% paraformaldehyde at room temperature for 30 minutes and stained with 1% crystal violet at room temperature for 20 minutes. Number of colonies was counted under an inverted microscope (Leica Microsystems GmbH, Wetzlar, Germany).

2.7 | Transwell migration and invasion assay

HeLa and C33A cells transfected with the indicated plasmids were collected and suspended in serum-free medium. Subsequently, 6×10^5 cells were added to the upper chamber covered with 25 mg Matrigel (BD Biosciences, Franklin Lakes, NJ, USA) in 100 mL PBS, the lower chamber was filled with medium containing 10% FBS. Following incubation at 37°C for 36 hours, cells below the membrane were fixed and stained with 0.5% crystal violet at room temperature for 15 minutes, washed with PBS, air-dried and observed under an inverted microscope (Olympus Corporation, Tokyo, Japan). Number of migrated and invaded cells was counted under a microscope.

2.8 | Flow cytometry analyses for apoptosis and cell cycle

At 48 hours after transfection, transfected HeLa and C33A cells were harvested by trypsinization and resuspended in cold PBS for analysis. For analysis of cell cycle, cells were stained with propidium iodide (PI; KeyGen, Beijing, China) according to the manufacturer's manual. Rate of cell apoptosis was detected using an Annexin V-FITC/PI apoptosis detection kit (KeyGen, Suzhou, China). These analyses were conducted according to the protocol provided by KeyGen Biotech (http://www.keygentec.com.cn).

2.9 | Enhanced green fluorescent protein reporter assay and Luciferase reporter assay

The hypothetical targets of miR-665 were predicted using TargetScan 7.2, miRDB and microRNA.org. Enhanced green fluorescent protein (EGFP) reporter plasmids with TGFBR1 3′UTR or TGFBR1 3′UTR mut and pri-miR-665 or ASO-miR-665 were transfected into HeLa and C33A cells with Lipofectamine 2000 reagent (Invitrogen), and red fluorescent protein (RFP) expressing plasmid was integrated as a transfection efficiency control. Cells were lysed 48 hours post-transfection, and the intensities of EGFP and RFP fluorescence were determined with a spectrophotometer. The hypothetical ceRNA of DANCR was predicted using RegRNA 2.0. The constructed pGL3-DANCR or pGL3-DANCR mut and the empty vectors were transfected into HeLa and C33A cells and the pRL-TK vectors was cotransfected as an internal control. At the indicated time points, luciferase assays were carried out with a Dual-Light Luciferase analysis system (Promega, Madison, WI, USA) according to the manufacturer's instructions.

2.10 | Immunofluorescence staining

HeLa cells transfected with specific plasmids were seeded in 24-well plates at the indicated time points before immunofluorescence staining. Cells were washed in PBS and fixed with 4% paraformaldehyde for 30 minutes at room temperature. After cells were washed with PBS, the cells were permeabilized using 0.25% Triton-X-100 for 5 minutes at room temperature and blocked in 10% donkey serum (Beyotime Biotechnology, Nanjing, China) for 30 minutes. The cells were subsequently incubated with primary antibodies against SMAD3 (1:200; Abcam, Cambridge, MA, USA) overnight at 4°C. The following day, cells were washed in PBS and then incubated at room temperature for 1 hour with a fluorescent-labeled secondary antibody (1:200; Beyotime Biotechnology), followed by incubation with DAPI (1:1000; Beyotime Biotechnology). Images were captured under a confocal microscope.

2.11 | In vivo tumorigenicity assay

Nude male BALB/c mice were used to determine tumorigenicity in vivo. Six-week-old female BALB/c athymic nude mice (Institute of Zoology, Chinese Academy of Sciences, Shanghai, China) were used (n = 18; divided into three groups; weight, 20-30 g; maintenance conditions: temperature, 18-29°C; relative humidity, 50%-60%; free access to clean food and water; and lighting for 10 hours [lights turned on at 8:00 every day and turned off at 18:00]). Stable-transfected HeLa cells were injected s.c. into the right flank near the forelimb. Tumor growth was measured every 5 days for 4 weeks. Tumor volumes were measured at different time-points using the formula: Tumor volume = length (mm) × width^2 (mm^2)/2. Mice were killed by cervical dislocation at the fourth week after s.c. injection. Tumor grafts were then excised and weighed.

2.12 | Western blot analysis

HeLa cells were lysed using the Protein Extraction kit according to the manufacturer's protocols (Beyotime Biotechnology). Total proteins (30 µg) were separated by 10% SDS-PAGE and transferred onto nitrocellulose membranes (EMD Millipore, Billerica, MA, USA). Membranes were blocked with 5% non-fat milk in Tris-buffered saline containing Tween-20 for ~2 hours at room temperature, prior to incubation with the primary antibodies. The membranes were probed with anti-E-cadherin (1:2000; Abcam), anti-ICAM1 (1:2000; Abcam), anti-Vimentin (1:2000; Abcam), anti-TGFBR1 (1:1000; Abcam), anti-p-ERK (1:2000; Abcam), anti-ERK (1:2000; Abcam), anti-SMAD2 (1:3000; Abcam), anti-p-SMAD2 (1:2000; Abcam), anti-SMAD2 (1:3000; Abcam), anti-p-SMAD3 (1:1000; Abcam), anti-SMAD3 (1:2000; Abcam), anti-p21 (1:3000; Abcam) and anti-GAPDH (1:3000; Abcam) antibodies overnight at 4°C. Subsequently, membranes were incubated with HRP-conjugated secondary antibody (1:3000; Cell Signaling Technology, Danvers, MA, USA) for 1 hour at 37°C. An ECL system (Thermo Fisher Scientific, Inc., Waltham, MA, USA) was used to detect the immunoreactive bands. Relative protein expression levels were normalized to that of GAPDH. Protein expression levels were measured using Image Pro Plus software v.6.0 (Media Cybernetics, Inc., Rockville, MD, USA).

2.13 | Statistical analysis

All analyses were carried out using SPSS 19 and GraphPad Prism 5.0. For comparisons of two treatment groups, Student's t test was used. For comparisons of three or more groups, one-way analysis of variance was followed by the Bonferroni post hoc test for comparison of two selected treatment groups; Dunnett's post hoc test was
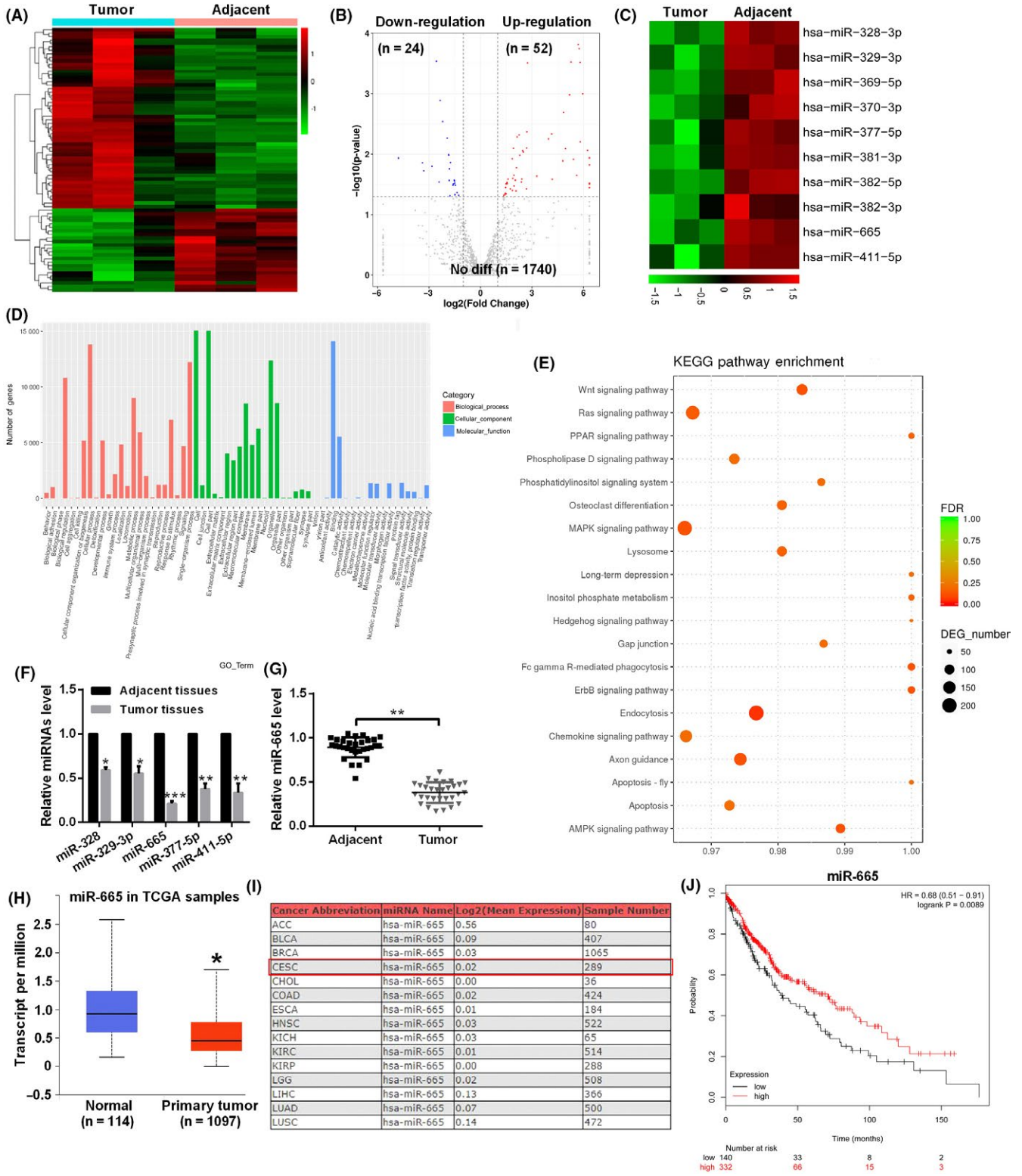
FIGURE 1 MicroRNA-665 (miR-665) was downregulated in cervical cancer (CC). A, Hierarchical clustering shows the miRNA array expression profile. B, Volcano plot shows the number of dysregulated miRNAs. C, Hierarchical clustering shows the top 10 downregulated miRNAs. D, Gene ontology (GO) analysis target genes of downregulated miRNAs. E, Statistics of pathway enrichment in dysregulated miRNAs. F, RT-qPCR assay shows levels of the indicated miRNAs. G, RT-qPCR assay shows the level of miR-665 in tumor tissues and adjacent tissues. H, The Cancer Genome Atlas (TCGA) database shows the level of miR-665 in cervical cancer patients and in control groups. I, OncomiR database shows the level of miR-665 in cervical cancer patients and in control groups. J, Kaplan Meier plotter software shows that patients with low miR-665 level had a poor prognosis. Experiments were carried out three times, and data are presented as means ± SD. *$P < .05$; **$P < .01$; ***$P < .001$

used for comparisons of the other treatment groups with the corresponding controls. Pearson's correlation analysis was used to determine the *r*-value. Associations between miR-655 expression and clinicopathological characteristics were assessed using chi-squared test. Pearson's chi-squared test was used to count the Pearson value using SPSS19.0. Data from at least three independent experiments are presented as means ± SD, or medians with ranges. *P* < .05 was considered to indicate a statistically significant difference.

3 | RESULTS

3.1 | MicroRNA-665 was downregulated in cervical cancer

To investigate the potential involvement of miRNAs in CC, we carried out high-throughput microarray assay for miRNAs using three paired samples of tumor tissues and the adjacent tissues (Figure 1A). Variation of miRNA expression is shown in the volcano plot and the results showed that 24 miRNAs were downregulated and 52 miRNAs were upregulated in CC tissues (Figure 1B). Hierarchical clustering also showed the top 10 downregulated miRNAs (Figure 1C). For further functional annotation, all predicted targets were analyzed by gene ontology (GO) terms and showed that 17 295 predicated targets were identified for the top 62 enriched GO categories in terms of cells, cellular components and binding activity (Figure 1D). Furthermore, KEGG pathway annotation showed that these target genes were significantly enriched in 20 canonical pathways, especially in metabolic pathways and tumorigenesis-related pathways (Figure 1E). RT-qPCR was used to verify the accuracy of the sequencing data, and the results showed that miR-665 was obviously downregulated compared with the other groups (Figure 1F). Furthermore, we also detected the level of miR-665 in 30 paired tissues and the results showed that miR-665 was downregulated in CC tissues (Figure 1G), which was negatively correlated with tumor size, distant metastasis and advanced TNM stage (Table 1). In addition, we analyzed the level of miR-665 in TCGA and the OncomiR database and found that the level of miR-665 was downregulated in CC patients (Figure 1H,I). Kaplan Meier plotter software showed that patients with a low miR-665 level had a poor prognosis (Figure 1J).

3.2 | MicroRNA-665 inhibited proliferation, migration and invasion in CC cells

In order to analyze the role of miR-665 on the progression of CC, the level of miR-665 was measured in CC cell lines. As shown in Figure 2A, miR-665 was significantly downregulated in HeLa, C33A, CasKi and SiHa cell lines compared with that in normal cervical cells. Transfection of pri-miR-665 into HeLa and C33A cells significantly increased the level of miR-665 and transfection of ASO-miR-665 into HeLa and C33A cells significantly decreased the level of miR-665 (Figure 2B). As hypothesized, we found that miR-665 overexpression led to cell growth inhibition at 48 and 72 hours through the MTT assay in HeLa and C33A cells

TABLE 1 Association between miR-665 expression and clinicopathological characteristics in cervical cancer

| Characteristic | n | miR-665 expression | | P |
		Low (n)	High (n)	
Age (y)				
≤50	18	9	9	
>50	12	9	3	0.171
TNM stage				
I/II	13	4	9	0.004[a]
III/IV	17	14	3	
Tumor size (cm)				
≤5	14	5	9	0.039[a]
>5	16	13	3	
Lymph node metastasis				
Absent	12	5	7	
Present	18	13	5	0.094
Distant metastasis				
Absent	15	5	10	
Present	15	13	2	0.003[a]
Histological grade				
Well	13	6	7	
Moderately/ Poorly	17	12	5	0.264

miR, microRNA; TNM, tumor node metastasis.
P-values in bold indicate statistically significant differences (*P* < 0.05).
[a]χ^2 test.

(Figure 2C). Further study of cell proliferation using colony formation assay also showed obvious attenuation of cell growth in HeLa and C33A cells transfected with pri-miR-665 (Figure 2D). To determine the role of miR-665 in the cell cycle of HeLa and C33A cells, flow cytometry was carried out to observe the distribution of the cell cycle after transfection of pri-miR-665 and ASO-miR-665. As shown in Figure 2E, upregulation of miR-665 induced a significant G_1-phase arrest in both HeLa and C33A cells, whereas downregulation of miR-665 significantly promoted cell proliferation by accelerating cell cycle progression in HeLa and C33A cells. In addition, our data showed that the apoptotic rate was significantly increased in cells transfected with pri-miR-665 and the apoptotic rate was significantly decreased in cells transfected with ASO-miR-665 (Figure 2F). Transwell assays showed that pri-miR-665 transfection prominently inhibited migration and invasion of HeLa and C33A cells and ASO-miR-665 transfection promoted the migration and invasion of HeLa and C33A cells (Figure 2G,H). Transfection of HeLa cells with pri-miR-665 caused decreased expression of vimentin and ICAM1 protein and increased expression of E-cadherin protein. In contrast, this result was reversed by treatment with ASO-miR-665 (Figure 2I). Furthermore, ectopic expression of miR-665 in HeLa and C33A cells inhibited the resistance for cisplatin in a time-dependent way (Figure 2J).
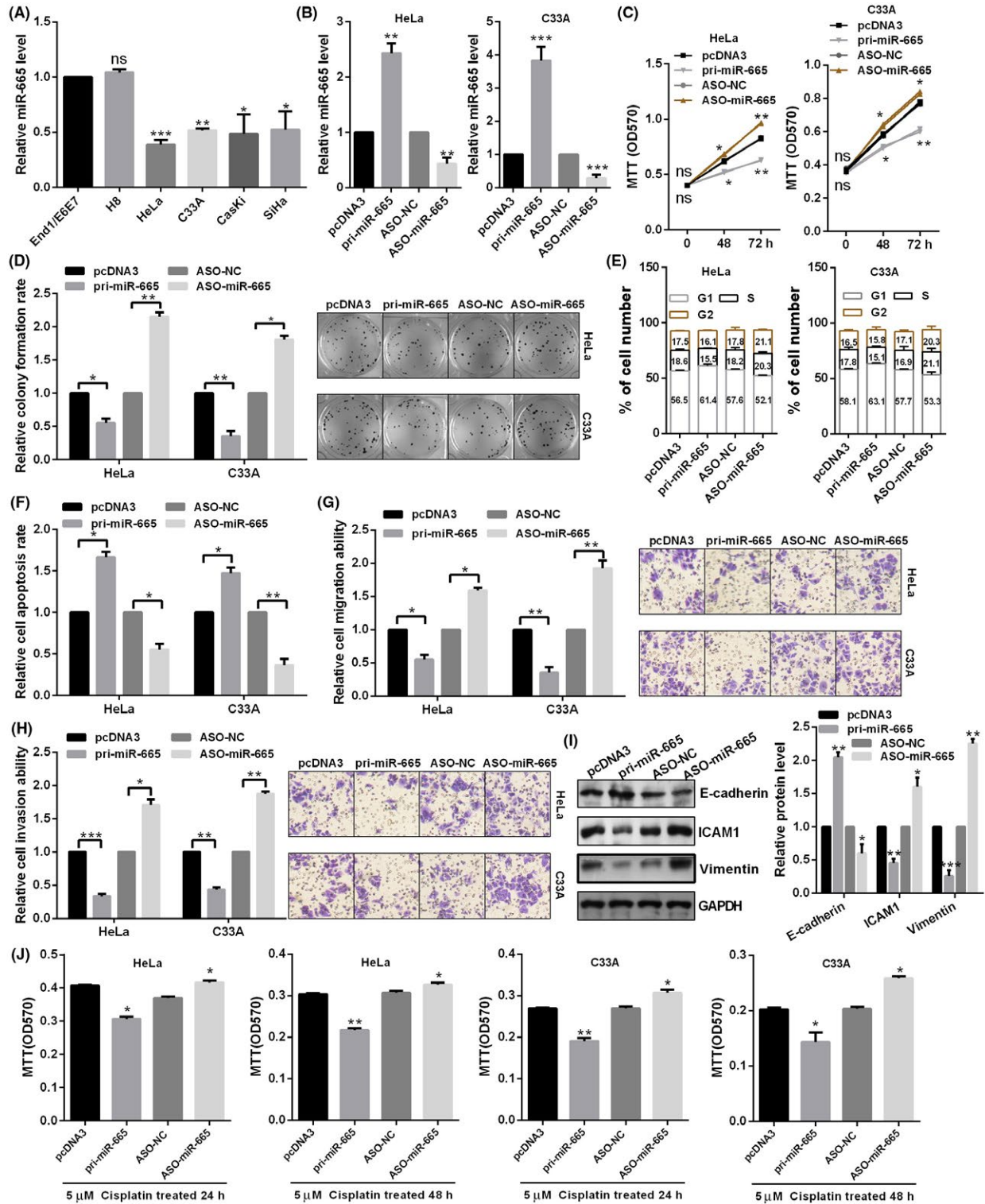
FIGURE 2 MicroRNA-665 (miR-665) functioned as a suppressor gene in cervical cancer (CC) cells. A, Expression levels of miR-665 in End1/E6E7, H8, HeLa, C33A, SiHa and CasKi cells were examined by RT-qPCR assay. B, Efficiency of pri-miR-665 or ASO-miR-665 was identified by RT-qPCR assay. C, Effect of miR-665 on HeLa and C33A cellular viabilities was determined by MTT assay. D, Relative colony formation rates of HeLa and C33A cells with indicated treatment were determined by colony formation assay. E, Flow cytometric cell cycle analysis shows that miR-665 overexpression results in a significant increase in the cellular population in the G_0/G_1 phase. F, Flow cytometric apoptosis shows that miR-665 overexpression significantly increased the apoptosis rate in HeLa and C33A cells. G,H, Transwell migration and invasion assays show that miR-665 suppressed cell migration and invasion ability. I, Western blot analysis of protein expression levels of E-cadherin, ICAM1 and vimentin following transfection with pri-miR-665 or ASO-miR-665 and the control groups in HeLa cells. J, miR-665 inhibited the drug resistance of HeLa and C33A cells to cisplatin. Experiments were carried out three times, and data are presented as means ± SD. *$P < .05$; **$P < .01$; ***$P < .001$; ns, not significant
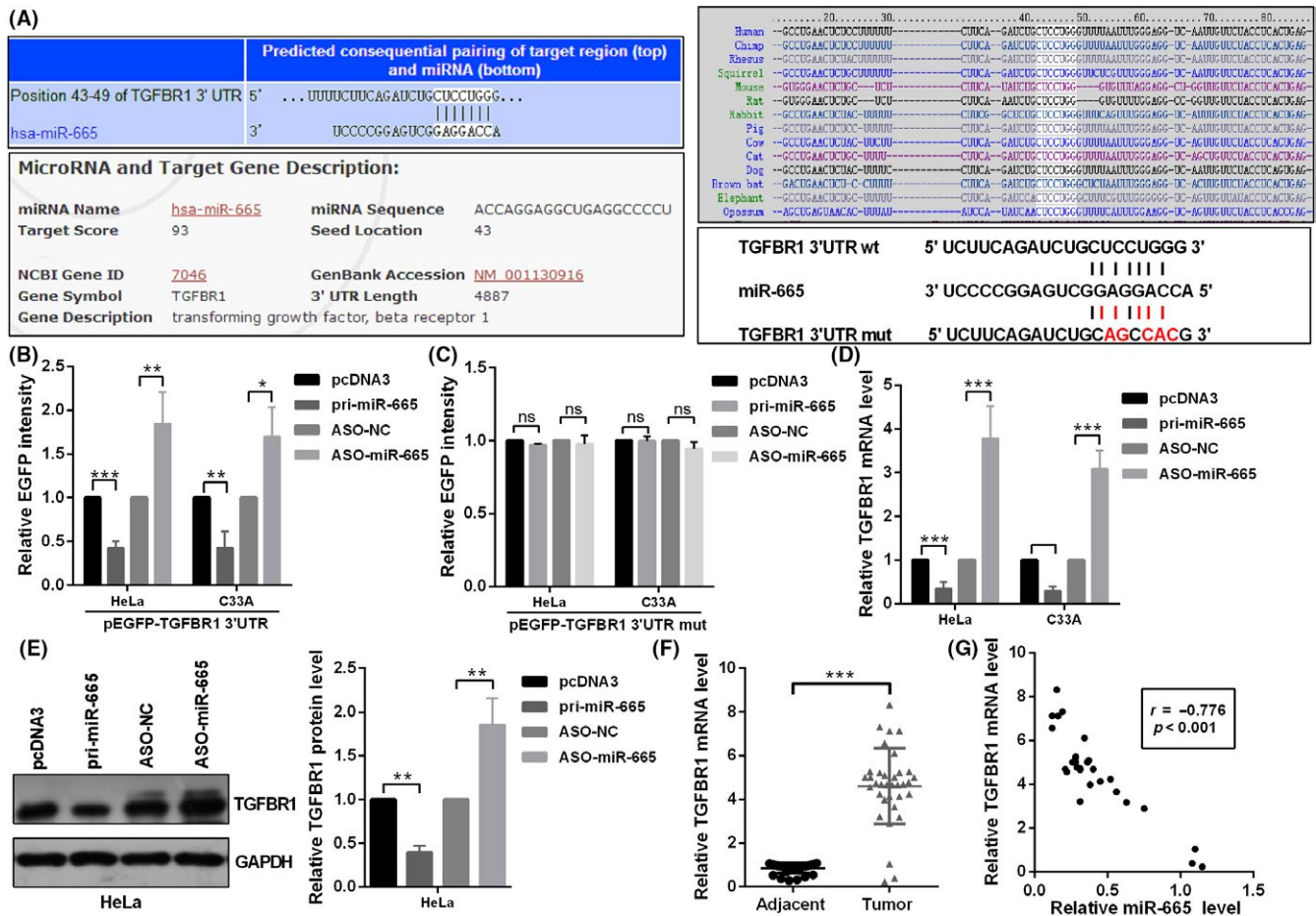
FIGURE 3 MicroRNA-665 (miR-665) directly targeted transforming growth factor beta receptor 1 (TGFBR1). A, Predicted miR-665 binding sites in TGFBR1 mRNA using TargetScan and miRDB are shown and the WT and the mutated 3′UTR of TGFBR1 mRNA are shown. B,C, enhanced green fluorescent protein intensity of HeLa and C33A cells expression in the WT or mutated 3′UTR of TGFBR1 was determined by spectrophotometry, and the value of the control group was set to 1. D, TGFBR1 mRNA expression levels in HeLa and C33A cells with indicated treatment were measured by RT-qPCR. E, TGFBR1 protein level in HeLa and C33A cells transfected with pri-miR-665 or ASO-miR-665 and respective controls were determined by western blot analysis. F, TGFBR1 mRNA levels in tumor tissues and adjacent tissues were detected by RT-qPCR assay. G, TGFBR1 mRNA expression level was negatively correlated with miR-665 level in tumor tissues. Experiments were carried out three times, and data are presented as means ± SD. *$P < .05$; **$P < .01$; ***$P < .001$; ns, not significant

3.3 | MicroRNA-665 directly targeted TGFBR1 in CC cells

To investigate the mechanism of miR-665 affecting the biological behavior of CC, we predicted the target genes of miR-665 using miRDB and TargetScanHuman 7.2. To verify that miR-665 can directly target TGFBR1 3′UTR, we constructed EGFP reporter plasmids containing the 3′UTR or the 3′UTR-mut of TGFBR1 (Figure 3A). In HeLa and C33A cells, relative EGFP activity was significantly reduced in both pri-miR-665 and wild-type (WT) 3′UTR of the TGFBR1 cotransfected group and cotransfection with ASO-miR-665 and wild-type 3′UTR of TGFBR1 increased relative EGFP activity (Figure 3B). However, EGFP activity was not almost changed when HeLa and C33A cells were cotransfected with pri-miR-665 or ASO-miR-665 and mutational EGFP reporter plasmid (Figure 3C). To further confirm the regulation of TGFBR1 by miR-665, RT-qPCR and western blot assays were carried out and the

results showed that pri-miR-665 markedly decreased the mRNA and protein levels of TGFBR1, and ASO-miR-665 increased the expression of TGFBR1 at the mRNA and protein levels (Figure 3D,E). In addition, we detected the level of TGFBR1 using RT-qPCR assay and found that TGFBR1 mRNA level was markedly upregulated in tumor tissues compared to the adjacent tissues (Figure 3F). Furthermore, using Pearson's correlation analysis, we also found that the mRNA level of TGFBR1 in tumor tissues was negatively correlated to the miR-665 level (Figure 3G). These data indicated that TGFBR1 is negatively regulated by miR-665 in CC cells, which is the novel target of miR-665.

3.4 | Overexpression of TGFBR1 rescued the phenotypes caused by miR-665 in CC cells

To determine the role of TGFBR1, we first detected the level of TGFBR1 in cervical cell lines and found that TGFBR1 was obviously

upregulated in CC cell lines compared with the control groups (Figure 4A). In addition, overexpression efficiency of TGFBR1 was confirmed by RT-qPCR and western blot assay (Figure 4B,C). By MTT analysis and colony formation analysis, we showed that TGFBR1 promoted cell growth rate, presented as increased OD570 value and colony formation number, whereas miR-665 could reverse the increased growth effects induced by TGFBR1 (Figure 4D,E). Flow cytometry analyses showed increased percentage of G_2/M cells and decreased percentage of G_0/G_1 cells upon overexpression of TGFBR1 compared with vector control, and the effects were neutralized by pri-miR-665 in HeLa and C33A cells (Figure 4F). Similarly, overexpression of TGFBR1 decreased the proportion of apoptotic cells only as compared with vector control and the opposite effect was observed by cotransfection pri-miR-665 and pTGFBR1 compared with overexpression of TGFBR1 only (Figure 4G). Transwell assay showed increased migration and invasion abilities upon TGFBR1 overexpression; however, when we carried out cotransfection with pri-miR-665 and pTGFBR1, all the effects we observed were neutralized by the addition of miR-665 (Figure 4H,I). Meanwhile, we carried out western blot to detect EMT markers to evaluate the effects of TGFBR1 in CC cells. TGFBR1 overexpression decreased the expression of epithelial cell marker E-cadherin and increased the mesenchymal cell marker vimentin and ICAM1, indicating that TGFBR1 promoted EMT progression (Figure 4J).

3.5 | MicroRNA-665 inactivated the ERK/SMAD pathway through TGFBR1

By western blot analyses, we showed that miR-665 inactivates the ERK/SMAD pathway as indicated by the suppressive expression of the phosphorylated form of ERK, SMAD2 and SMAD3, and p21, but with no changes for total expression of ERK, SMAD2 and SMAD3 (Figure 5A). However, combination treatments of miR-665 and TGFBR1 had no effects on this pathway. To detect the distribution of SMAD3, immunofluorescent assays were carried out in HeLa cells. Results showed that overexpression of miR-665 decreased the nuclear distribution of SMAD3 in HeLa cells. Cotransfection with pri-miR-665 and pTGFBR1 partly rescued the effects of miR-665 overexpression (Figure 5B).

3.6 | MicroRNA-665 inhibited tumor growth through TGFBR1

To investigate the effects of miR-665 on the tumor growth in vivo, HeLa cells were transfected with pcDNA3 plus pcDNA3, pcDNA3 plus pri-miR-665, and pri-miR-665 plus pTGFBR1 s.c. injected into nude mice (Figure 5C). Our results showed that tumors from pri-miR-665 transfected HeLa cells grew more slowly than those from the control group or the pri-miR-665 and pTGFBR1 cotreatment group during the entire tumor growth period (Figure 5D). Average weights of tumors derived from pri-miR-665-transfected HeLa cells were significantly smaller than those of the control group or the pri-miR-665 and pTGFBR1 cotreatment group (Figure 5E).

3.7 | Long noncoding-DANCR acts as a molecular sponge for miR-665 in CC cells

According to the RegRNA 2.0 database, we found that lnc-DANCR carries putative miR-665 targeting sites (Figure 6A). Next, we constructed the reporter vector containing WT or mutant miR-665 putative binding sites in lnc-DANCR (Figure 6B). Overexpression of miR-665 decreased and ASO-miR-665 increased the fluorescence intensity of cells transfected with the WT reporter vector, whereas further use of lnc-DANCR mut had no influence (Figure 6C,D). Enhanced expression of miR-665 resulted in significant downregulation of lnc-DANCR, whereas knockdown of miR-665 obviously increased the expression level of lnc-DANCR in HeLa and C33A cells (Figure 6E). In addition, transfection efficiency of the overexpression plasmid for lnc-DANCR was detected by RT-qPCR assay in HeLa and C33A cells (Figure 6F). Ectopic expression of lnc-DANCR significantly increased TGFBR1 expression at mRNA and protein level in HeLa and C33A cells. However, we did not observe a significant difference in TGFBR1 level after transfection with lnc-DANCR and pri-miR-665 (Figure 6G,H). We detected the level of DANCR in tissues and found that the level of DNACR in tumor tissues was upregulated compared with the adjacent normal tissues (Figure 6I). Furthermore, using Pearson's correlation analysis, we also found that the mRNA level of TGFBR1 in tumor tissues was positively correlated with the lnc-DANCR level (Figure 6J). Finally, Kaplan Meier plotter software showed that patients with high TGFBR1 level had a poor prognosis (Figure 6K).

FIGURE 4 Transforming growth factor beta receptor 1 (TGFBR1) promoted cell proliferation and epithelial-mesenchymal transition (EMT). A, Expression levels of TGFBR1 in End1/E6E7, H8, HeLa, C33A, SiHa and CasKi cells were examined by RT-qPCR assay. B,C, RT-qPCR and western blot assay show the efficiency of the overexpression plasmid of TGFBR1 in HeLa and C33A cells. D, Indicated transfection on HeLa and C33A cellular viabilities was determined by MTT assay. HeLa and C33A cells were transfected with the indicated combinations of pcDNA3 and pTGFBR1 or pri-miR-665 and pTGFBR1 or the control group. E, Relative colony formation rates of HeLa and C33A cells with the indicated transfection were determined by colony formation assay. TGFBR1 overexpression promoted colony formation ability. F, Flow cytometry cell cycle assay shows the indicated transfection on the cell cycle in HeLa and C33A cells. TGFBR1 overexpression increased the number of HeLa and C33A cells in the S and G_2 phases and decreased the number of cells in G_1 phase. G, Flow cytometry apoptosis assay shows the indicated transfection on apoptosis in HeLa and C33A cells. TGFBR1 overexpression inhibited cell apoptosis. H,I, Transwell migration and invasion assays show that pri-miR-665 and TGFBR1 rescued TGFBR1-mediated cell migration and invasion ability in HeLa and C33A cells. J, Western blot assays show protein levels of E-cadherin, ICAM1 and vimentin after transfection with the indicated plasmids in HeLa and C33A cells. Experiments were carried out three times, and data are presented as means ± SD. *$P < .05$; **$P < .01$; ***$P < .001$; ns, not significant
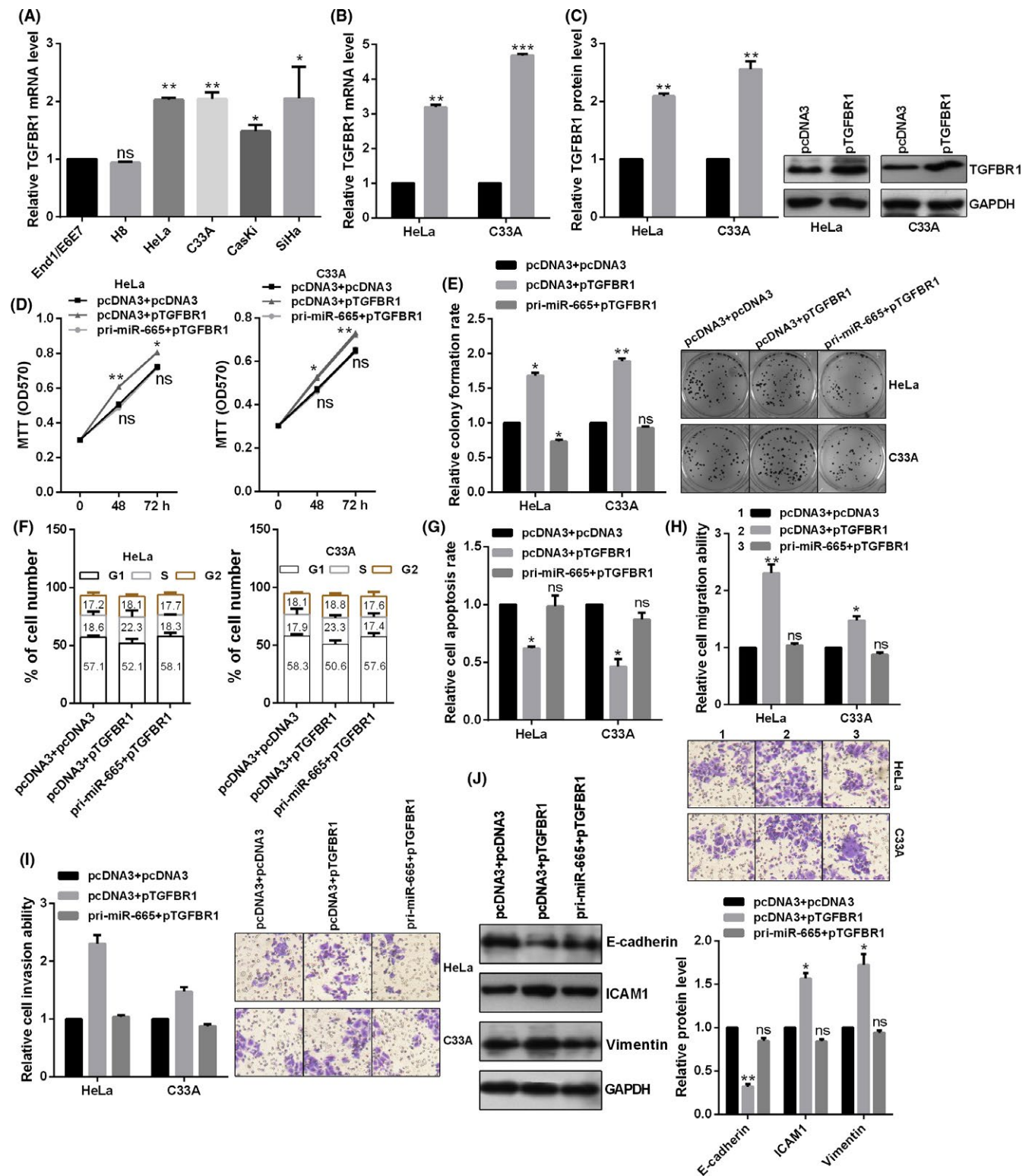
4 | DISCUSSION

In recent years, many studies have reported that lncRNAs can function as ceRNA to regulate the expression of miRNAs in many cancers.[21-23] For example, Li et al[24] reported that lncRNA NCK1-AS1 promotes proliferation and induces cell cycle progression by regulating the NCK1-AS1/miR-6857/CDK1 pathway in CC cells.

In addition, Yu et al[25] reported that lncRNA HCP5 promotes the development of cervical cancer by regulating MACC1 by suppression of miRNA-15a. Furthermore, Guo et al[26] reported that lncRNA SNHG20 promotes cell proliferation and invasion by the miR-140-5p-ADAM10 axis in cervical cancer. Recently, many studies have reported that lnc-DANCR plays an important role in esophageal cancer,[27] glioma,[28] osteosarcoma,[29] colorectal cancer,[30] cervical
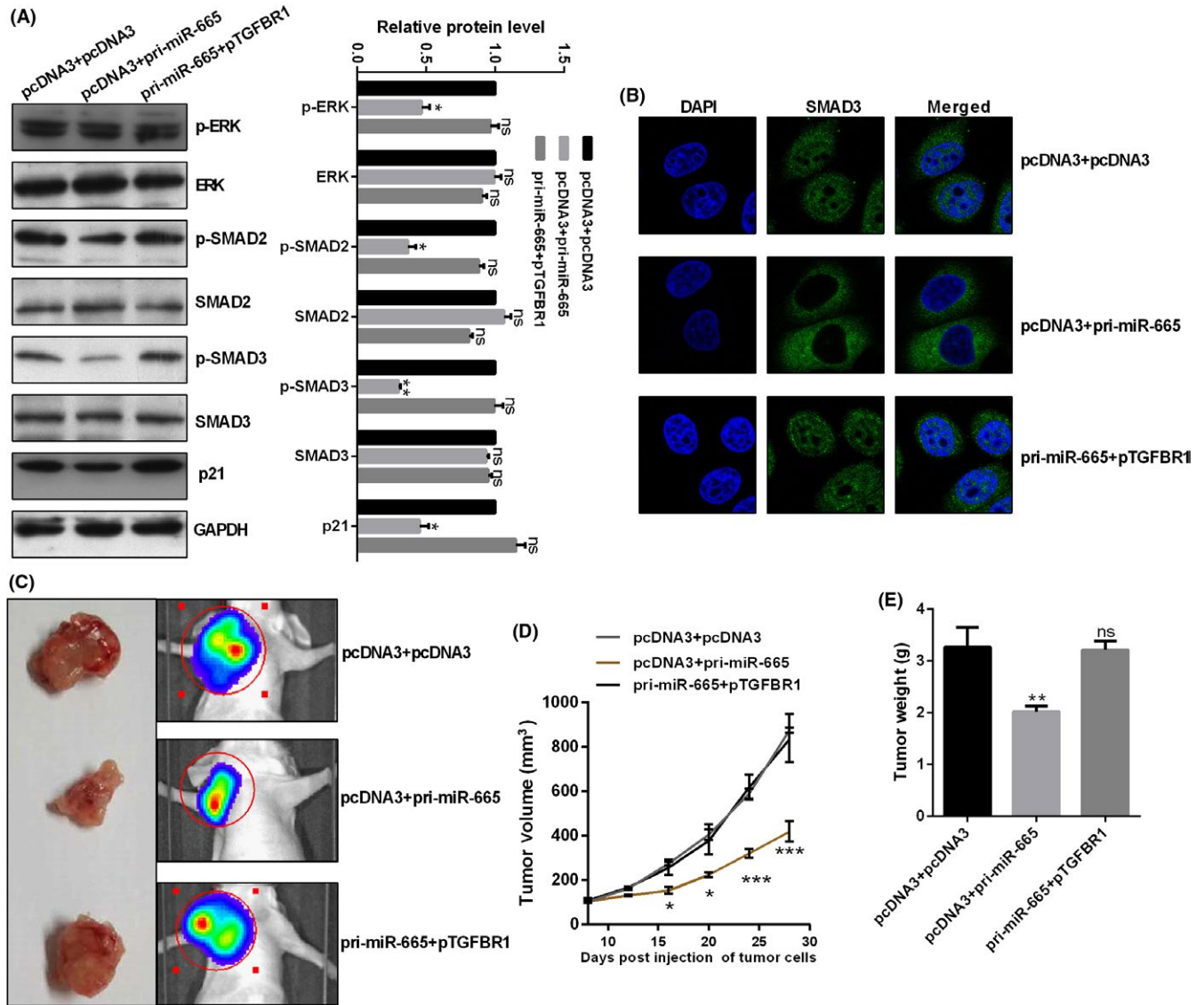
FIGURE 5 MicroRNA-665 (miR-665) inhibited the ERK/SMAD pathway and tumor growth in vivo through transforming growth factor beta receptor 1 (TGFBR1). A, Western blot assay shows the protein levels of p-ERK, ERK, p-SMAD2, SMAD2, p-SMAD3, SMAD3 and p21 transfected with pcDNA3 + pri-miR-665, pri-miR-665 + pTGFBR1 and the control group in HeLa cells. B, Immunofluorescent assay shows the distribution of SMAD3 transfected with the indicated plasmids in HeLa cells. miR-665 inhibited but TGFBR1 promoted the nuclear distribution of SMAD3 in HeLa cells. C, Compared with the control group, the tumorigenic ability of HeLa cells was inhibited after transfection with miR-665 and the tumorigenic ability of HeLa cells was rescued after transfection with miR-665 and TGFBR1. D, Tumor growth rate was significantly decreased after treatment with pri-miR-665. E, miR-665 inhibited tumor weight. Experiments were carried out three times, and data are presented as means ± SD. *$P < .05$; **$P < .01$; ***$P < .001$; ns, not significant

cancer,[31] and so on. Recently, Liang et al reported that lnc-DANCR promoted cervical cancer progression by upregulating ROCK1 through sponging miR-335-5p.[32] In present study, we showed that lnc-DANCR functions as a ceRNA of miR-665 to regulate CC progression. Hence, the previous study and our present results indicate that lnc-DNACR could be a target for the future prevention and therapeutics of cervical cancer.

MicroRNA-665 was downregulated in ovarian cancer,[33] pancreatic cancer,[34] hepatocellular carcinoma,[35] inflammatory bowel disease,[36] and so on. However, the role and mechanism of miR-665 in CC remains unknown. In the present study, using microarray

sequencing, TCGA and the OncomiR database we found that miR-665 was downregulated in CC, level of miR-665 was negatively correlated with tumor size, distant metastasis, advanced TNM stage and poor prognosis. Function analysis showed that miR-665 overexpression inhibited cell proliferation in CC cells in vitro and tumor growth in vivo. Next, Transwell analysis showed that the inhibitive effect of miR-665 on cell migration and invasion occurred by blocking EMT in CC cells. In addition, miR-665 overexpression also inhibited the cell cycle process, drug resistance and promoted cell apoptosis. Furthermore, we found miR-665 could inactivate the ERK/SMAD pathway in CC cells.
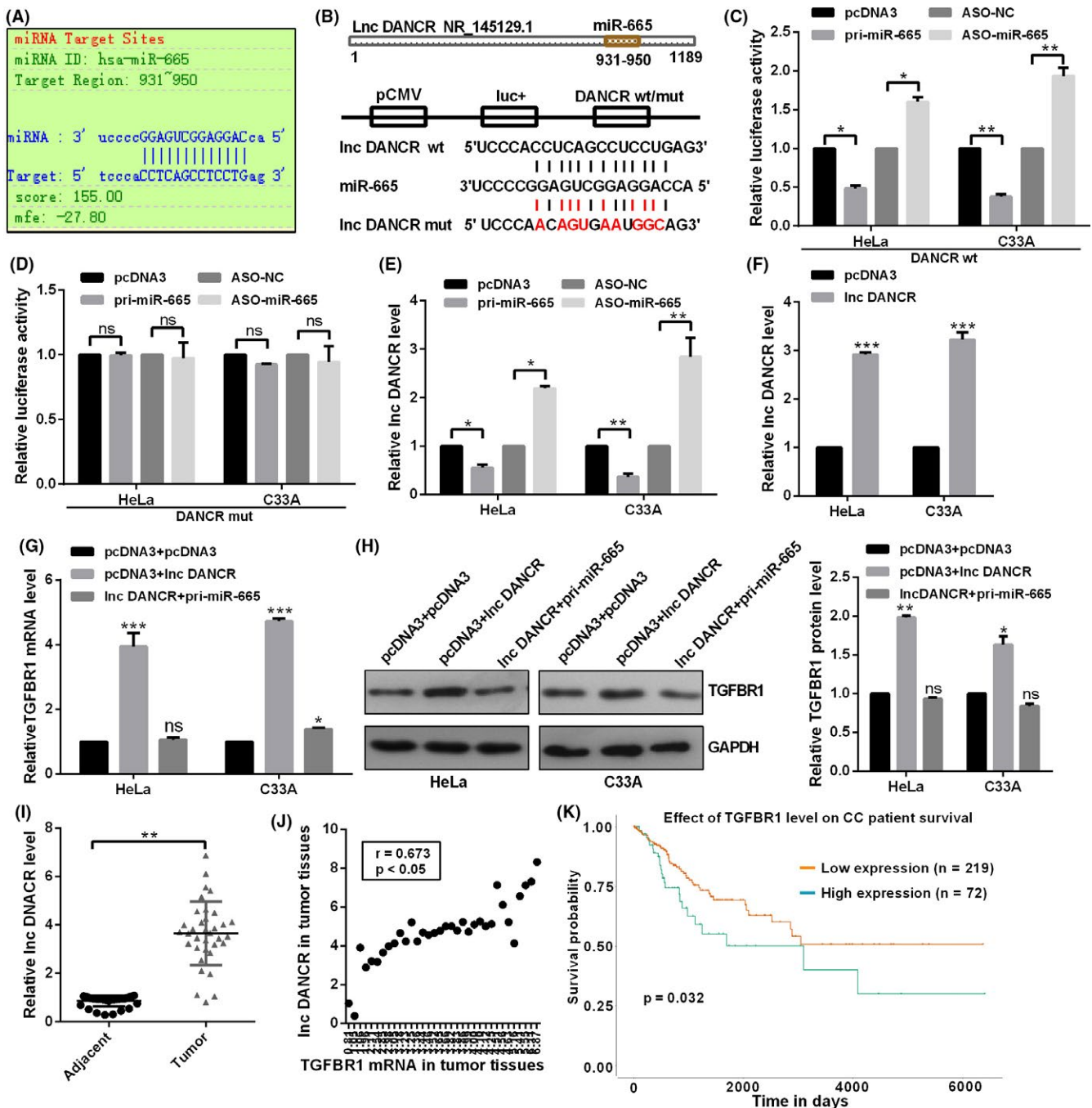
FIGURE 6 Long noncoding (lnc)-DANCR acted as a molecular sponge for microRNA-665 (miR-665) in cervical cancer (CC) cells. A, Information of miR-665 and lnc-DANCR is shown using RegRNA 2.0 software. B, Putative and mutant binding sites of miR-665 on lnc-DANCR are shown. C,D, Fluorescence intensity was measured in HeLa and C33A cells cotransfected with pri-miR-665 or ASO-miR-665 and DANCR WT or mutant construct. E, RT-qPCR was used to assess lnc-DANCR levels in HeLa and C33A cells in response to altered miR-665 expression. F, RT-qPCR shows the expression level of miR-665 when the expression of lnc-DANCR was enhanced or suppressed. G,H, lnc-DANCR promoted transforming growth factor beta receptor 1 (TGFBR1) mRNA and protein levels in HeLa and C33A cells by sponging miR-665. I, RT-qPCR assay shows the level of lnc-DANCR in patients and in control groups. J, TGFBR1 mRNA expression level was positively correlated with DANCR level in tumor tissues. K, Kaplan Meier plotter software shows that patients with high TGFBR1 level had a poor prognosis. Experiments were carried out three times, and data are presented as means ± SD. *$P < .05$; **$P < .01$; ***$P < .001$; ns, not significant

It is well known that miRNAs may directly target the 3′UTR of mRNAs and lead to mRNA decay or translation suppression.[37] We found that miR-665 could directly target TGFBR1 in HeLa and C33A

cells. Moses et al reported that TGFβ binds to the heterodimeric type II and type I TGF-β serine/threonine kinase receptors (TGFBR2 and TGFBR1) and initiates a signaling cascade through phosphorylation

of SMAD2 and SMAD3.[38,39] TGFBR1 promoted cell proliferation, migration and invasion in lung cancer,[40] pancreatic cancer,[41] and glioblastoma.[42] In this study, we reported that TGFBR1 promoted cell proliferation, migration, invasion and the cell cycle and inhibit cell apoptosis in HeLa and C33A cells. Furthermore, TGFBR1 overexpression could attenuate the inhibitive role of miR-665 on the ERK/SMAD pathway in cervical cancer cells.

In conclusion, the present study showed that miR-665 was downregulated in cervical cancer, and overexpression of miR-665 could inhibit growth and metastasis of cervical cancer. Our study elucidated a novel pathway in lnc-DANCR-mediated miR-665 targeting TGFBR1 on growth and metastasis, which suggests new therapeutic targets, including the ERK/SMAD signaling pathway, in the prevention and treatment of cervical cancer.

ACKNOWLEDGMENT

CONFLICTS OF INTEREST

Authors declare no conflicts of interest for this article.

ORCID

Lixin Dong https://orcid.org/0000-0002-0241-8959

REFERENCES

1. Lea JS, Lin KY. Cervical cancer. *Obstet Gynecol Clin North Am*. 2012;39:233-253.
2. Torre LA, Bray F, Siegel RL, Ferlay J, Lortet-Tieulent J, Jemal A. Global cancer statistics, 2012. *CA Cancer J Clin*. 2015;65:87-108.
3. Huang P, Xi J, Liu S. MiR-139-3p induces cell apoptosis and inhibits metastasis of cervical cancer by targeting NOB1. *Biomed Pharmacother*. 2016;83:850-856.
4. Chen W, Zheng R, Baade PD, et al. Cancer statistics in China, 2015. *CA Cancer J Clin*. 2016;66:115-132.
5. Rafiee A, Riazi-Rad F, Havaskary M, Nuri F. Long noncoding RNAs: regulation, function and cancer. *Biotechnol Genet Eng Rev*. 2018;34(2):153-180.
6. Shi D, Zhang C, Liu X. Long noncoding RNAs in cervical cancer. *J Cancer Res Ther*. 2018;14(4):745-753.
7. Chen J, Liu S, Hu X. Long non-coding RNAs: crucial regulators of gastrointestinal cancer cell proliferation. *Cell Death Discov*. 2018;4:50.
8. Thin KZ, Liu X, Feng X, Raveendran S, Tu JC. LncRNA-DANCR: a valuable cancer related long non-coding RNA for human cancers. *Pathol Res Pract*. 2018;214(6):801-805.
9. Zhan Y, Chen Z, Li Y, et al. Long non-coding RNA DANCR promotes malignant phenotypes of bladder cancer cells by modulating the miR-149/MSI2 axis as a ceRNA. *J Exp Clin Cancer Res*. 2018;37(1):273.
10. Yang XJ, Zhao JJ, Chen WJ, Zhang GG, Wang W, Tao HC. Silencing long non-coding RNA, differentiation antagonizing non-protein coding RNA promotes apoptosis and inhibits tumor growth in colon cancer. *Oncol Lett*. 2018;16(3):2865-2872.
11. Lu Y, Hu Z, Mangala LS, et al. MYC targeted long noncoding RNA DANCR promotes cancer in part by reducing p21 levels. *Cancer Res*. 2018;78(1):64-74.
12. Lee RC, Feinbaum RL, Ambros V. The *C. elegans* heterochronic gene lin-4 encodes small RNAs with antisense complementarity to lin-14. *Cell*. 1993;75:843-854.
13. Zhang H, Li T, Zheng L, Huang X. Biomarker microRNAs for diagnosis of oral squamous cell carcinoma identified based on gene expression data and microRNA-mRNA network analysis. *Comput Math Methods Med*. 2017;2017:9803018.
14. Babashah S, Bakhshinejad B, Birgani MT, Pakravan K, Cho WC. Regulation of microRNAs by phytochemicals: a promising strategy for cancer chemoprevention. *Curr Cancer Drug Targets*. 2018;18:640-651.
15. Li J, Liu Q, Clark LH, Qiu H, Bae-Jump VL, Zhou C. Deregulated miRNAs in human cervical cancer: functional importance and potential clinical use. *Future Oncol*. 2017;13:743-753.
16. Laengsri V, Kerdpin U, Plabplueng C, Treeratanapiboon L, Nuchnoi P. Cervical cancer markers: epigenetics and microRNAs. *Lab Med*. 2018;49:97-111.
17. Shishodia G, Verma G, Das BC, Bharti AC. miRNA as viral transcription tuners in HPV-mediated cervical carcinogenesis. *Front Biosci*. 2018;10:21-47.
18. Li GC, Cao XY, Li YN, et al. MicroRNA-374b inhibits cervical cancer cell proliferation and induces apoptosis through the p38/ERK signaling pathway by binding to JAM-2. *J Cell Physiol*. 2018;233:7379-7390.
19. Lu HJ, Jin PY, Tang Y, et al. microRNA-136 inhibits proliferation and promotes apoptosis and radiosensitivity of cervical carcinoma through the NF-kappaB pathway by targeting E2F1. *Life Sci*. 2018;199:167-178.
20. Guo J, Yang Z, Yang X, Li T, Liu M, Tang H. miR-346 functions as a pro-survival factor under ER stress by activating mitophagy. *Cancer Lett*. 2018;413:69-81.
21. Kondo Y, Shinjo K, Katsushima K. Long non-coding RNAs as an epigenetic regulator in human cancers. *Cancer Sci*. 2017;108:1927-1933.
22. Lekka E, Hall J. Noncoding RNAs in disease. *FEBS Lett*. 2018;592:2884-2900.
23. Yang S, Sun Z, Zhou Q, et al. MicroRNAs, long noncoding RNAs, and circular RNAs: potential tumor biomarkers and targets for colorectal cancer. *Cancer Manag Res*. 2018;10:2249-2257.
24. Li H, Jia Y, Cheng J, Liu G, Song F. LncRNA NCK1-AS1 promotes proliferation and induces cell cycle progression by crosstalk NCK1-AS1/miR-6857/CDK1 pathway. *Cell Death Dis*. 2018;9:198.
25. Yu Y, Shen HM, Fang DM, Meng QJ, Xin YH. LncRNA HCP5 promotes the development of cervical cancer by regulating MACC1 via suppression of microRNA-15a. *Eur Rev Med Pharmacol Sci*. 2018;22:4812-4819.
26. Guo H, Yang S, Li S, Yan M, Li L, Zhang H. LncRNA SNHG20 promotes cell proliferation and invasion via miR-140-5p-ADAM10 axis in cervical cancer. *Biomed Pharmacother*. 2018;102:749-757.
27. Shi H, Shi J, Zhang Y, et al. Long non-coding RNA DANCR promotes cell proliferation, migration, invasion and resistance to apoptosis in esophageal cancer. *J Thorac Dis*. 2018;10:2573-2582.
28. Yang JX, Sun Y, Gao L, Meng Q, Yang BY. Long non-coding RNA DANCR facilitates glioma malignancy by sponging miR-33a-5p. *Neoplasma*. 2018;65:790-798.
29. Wang Y, Zeng X, Wang N, et al. Long noncoding RNA DANCR, working as a competitive endogenous RNA, promotes ROCK1-mediated proliferation and metastasis via decoying of miR-335-5p and miR-1972 in osteosarcoma. *Mol Cancer*. 2018;17:89.
30. Wang Y, Lu Z, Wang N, et al. Long noncoding RNA DANCR promotes colorectal cancer proliferation and metastasis via miR-577 sponging. *Exp Mol Med*. 2018;50:57.

31. Liang H, Zhang C, Guan H, Liu J, Cui Y. LncRNA DANCR promotes cervical cancer progression by upregulating ROCK1 via sponging miR-335-5p. *J Cell Physiol*. 2018. [Epub ahead of print]. https://doi.org/10.1002/jcp.27484

32. Zhen Q, Gao LN, Wang RF, et al. LncRNA DANCR promotes lung cancer by sequestering miR-216a. *Cancer Control*. 2018;25:1073274818769849.

33. Liu J, Jiang Y, Wan Y, Zhou S, Thapa S, Cheng W. MicroRNA665 suppresses the growth and migration of ovarian cancer cells by targeting HOXA10. *Mol Med Rep*. 2018;18:2661-2668.

34. Zhou B, Guo W, Sun C, Zhang B, Zheng F. Linc00462 promotes pancreatic cancer invasiveness through the miR-665/TGFBR1-TGFBR2/SMAD2/3 pathway. *Cell Death Dis*. 2018;9:706.

35. Qu Z, Wu J, Wu J, et al. Exosomal miR-665 as a novel minimally invasive biomarker for hepatocellular carcinoma diagnosis and prognosis. *Oncotarget*. 2017;8:80666-80678.

36. Li M, Zhang S, Qiu Y, et al. Upregulation of miR-665 promotes apoptosis and colitis in inflammatory bowel disease by repressing the endoplasmic reticulum stress components XBP1 and ORMDL3. *Cell Death Dis*. 2017;8:e2699.

37. Romero-Cordoba SL, Salido-Guadarrama I, Rodriguez-Dorantes M, Hidalgo-Miranda A. miRNA biogenesis: biological impact in the development of cancer. *Cancer Biol Ther*. 2014;15:1444-1455.

38. Moses HL, Roberts AB, Derynck R. The discovery and early days of TGF-beta: A historical perspective. *Cold Spring Harb Perspect Biol*. 2016;8:pii: a021865.

39. Zhao Y, Wang X, Wang Q, et al. USP2a supports metastasis by tuning TGF-beta signaling. *Cell Rep*. 2018;22:2442-2454.

40. Yang Z, He J, Gao P, et al. miR-769-5p suppressed cell proliferation, migration and invasion by targeting TGFBR1 in non-small cell lung carcinoma. *Oncotarget*. 2017;8:113558-113570.

41. Mody HR, Hung SW, Pathak RK, Griffin J, Cruz-Monserrate Z, Govindarajan R. miR-202 diminishes TGFbeta receptors and attenuates TGFbeta1-induced EMT in pancreatic cancer. *Mol Cancer Res*. 2017;15:1029-1039.

42. He X, Liu Z, Peng Y, Yu C. MicroRNA-181c inhibits glioblastoma cell invasion, migration and mesenchymal transition by targeting TGF-beta pathway. *Biochem Biophys Res Commun*. 2016;469:1041-1048.